



HAL
open science

A method to quantify intracellular glycation in dermal fibroblasts using liquid chromatography coupled to fluorescence detection – Application to the selection of deglycation compounds of dermatological interest

Amandine André, Joanna Wdzieczak-Bakala, Alexis Kaatio Touré, Didier Stien, Véronique Eparvier

► To cite this version:

Amandine André, Joanna Wdzieczak-Bakala, Alexis Kaatio Touré, Didier Stien, Véronique Eparvier. A method to quantify intracellular glycation in dermal fibroblasts using liquid chromatography coupled to fluorescence detection – Application to the selection of deglycation compounds of dermatological interest. *Journal of Chromatography B - Analytical Technologies in the Biomedical and Life Sciences*, 2018, 1100-1101, pp.100-105. 10.1016/j.jchromb.2018.09.034 . hal-01974037

HAL Id: hal-01974037

<https://hal.sorbonne-universite.fr/hal-01974037>

Submitted on 8 Jan 2019

HAL is a multi-disciplinary open access archive for the deposit and dissemination of scientific research documents, whether they are published or not. The documents may come from teaching and research institutions in France or abroad, or from public or private research centers.

L'archive ouverte pluridisciplinaire **HAL**, est destinée au dépôt et à la diffusion de documents scientifiques de niveau recherche, publiés ou non, émanant des établissements d'enseignement et de recherche français ou étrangers, des laboratoires publics ou privés.

1
2
3
4 **A method to quantify intracellular glycation in dermal fibroblasts using**
5 **liquid chromatography coupled to fluorescence detection – Application to**
6 **the selection of deglycation compounds of dermatological interest**
7
8
9

10 Amandine André^{a,b}, Joanna Wdzieczak-Bakala^a, Alexis Kaatio Touré^b, Didier Stien^c and
11 Véronique Eparvier^a
12

13
14 ^aCNRS, Institut de Chimie des Substances Naturelles UPR 2301, Université Paris-Saclay, Gif-Sur-
15 Yvette, France

16 ^bLaboratoire Shigeta, Paris, France

17 ^cCNRS, Laboratoire de Biodiversité et Biotechnologies Microbiennes, Observatoire
18 océanologique, Sorbonne Universités, Banyuls-Sur-Mer, France
19
20
21

22 Corresponding author:

23 A. André^{a,b}, ^aCNRS, Institut de Chimie des Substances Naturelles UPR 2301, Avenue de la
24 Terrasse, 91190 Gif-Sur-Yvette, France, ^bLaboratoire Shigeta, 62 boulevard Davout, 75020 Paris,
25 France, amandine.andre@cnrs.fr, 0169823610.
26
27
28

29 J. Wdzieczak-Bakala^a, ^aCNRS, Institut de Chimie des Substances Naturelles UPR 2301, Avenue de
30 la Terrasse, 91190 Gif-Sur-Yvette, France, johanna.bakala@cnrs.fr.
31
32

33 K. Touré^b, ^bLaboratoire Shigeta, 62 boulevard Davout, 75020 Paris, France, ktoure@shigeta.fr.
34

35 D. Stien^c, ^cCNRS, Laboratoire de Biodiversité et Biotechnologies Microbiennes, Sorbonne
36 Universités, Observatoire océanologique, 66650 Banyuls-Sur-Mer, France, didier.stien@cnrs.fr.
37
38

39 V. Eparvier^a, ^aCNRS, Institut de Chimie des Substances Naturelles UPR 2301, Avenue de la
40 Terrasse, 91190 Gif-Sur-Yvette, France, veronique.eparvier@cnrs.fr.
41
42
43
44
45
46
47
48
49
50
51
52
53
54
55
56
57
58
59
60

61
62
63 **Abstract**
64

65 Glycation is a common non-enzymatic reaction between proteins and sugars, which
66 gives rise in the human body to the formation of advanced glycation end products
67 (AGEs). These modifications impacts both extra and intracellular proteins, leading to
68 cells and tissues dysfunctions. In the skin, accumulation of AGEs leads to aesthetic
69 consequences, wrinkles, dark spots and yellowish skin tone, as it can be seen in diabetic
70 patients. Consequently, there is a growing dermatological interest to find compounds
71 able to eliminate AGEs accumulated in skin.
72
73

74 In this context, a method has been developed to detect and quantify intracellular
75 glycation in human dermal fibroblasts. After cultivation of fibroblasts, cell lysates were
76 injected in an HPLC system coupled with a fluorescence detector in by-pass mode. The
77 system allows the simultaneous measurement of global AGEs and particular
78 pentosidine amounts using two sets of wavelengths in a single run of one minute. The
79 immunocytochemistry approach was used to valid the HPLC analysis data.
80
81

82 The method developed was able to quantify changes in global AGEs and pentosidine
83 content in cells in response to glyoxal treatment. Fibroblasts treated with 500 μ M of
84 glyoxal for 48 hours showed a significant 2.3-fold and 2.6-fold increase in the content of
85 AGEs and pentosidine respectively compared to control cells.
86
87

88 As an application, a screening of natural extracts have been done and the method
89 allowed identifying extracts able to significantly reduce the amount of pentosidine in
90 fibroblasts (- 32 %). These extracts act as deglycation agents of interest in the field of
91 dermatology and cosmetology.
92
93

94 **Keywords:** Advanced glycation End product (AGEs), HPLC, Fluorescence, Human
95 Dermal Fibroblasts, Immunocytochemistry, Deglycation
96
97
98
99
100
101
102
103
104
105
106
107
108
109
110
111
112

1. Introduction

The glycation process, discovered by Maillard in 1912 [1], is a non-enzymatic transformation involving reducing sugars and amino-acids residues of proteins, leading to the formation of a complex and heterogeneous group of compounds named advanced glycation end products (AGEs). More precisely, the process of glycation involves first the reaction of an ose (mainly glucose) with an amine group of a protein amino acid (like lysine or arginine), to form a Schiff base. An Amadori molecular rearrangement then leads to the irreversible formation of AGEs by successive cyclisation and oxidation reactions (Fig. 1.). Due to the various reactions leading to their creation, multiple AGEs have been detected in tissues, and can be divided into three categories: fluorescent AGEs forming reticulations between proteins (for example: pentosidine, crossline), non-fluorescent AGEs forming reticulations between proteins (for example: glyoxal-lysine dimer (GOLD), methylglyoxal-lysine dimer (MOLD)), and fluorescent or non-fluorescent AGEs forming adducts on proteins (for example: *N*- ϵ -carboxymethyllysine (CML), pyrrolaline)[2].

AGEs accumulate during the lifetime in whole body including blood plasma, extracellular fluids and cells [3]. Consequently, they are considered as the main causing agent of numerous age-related diseases [4] such as diabetic vascular complications [5], atherosclerosis [6] or Alzheimer's disease [3, 7]. Long lifespan proteins of the body like hemoglobin, collagen or elastin, are known targets of irreversible modifications due to AGEs formation [4]. Extracellular proteins cross-linking leads to cell growth inhibition, impaired cell adhesion and tissue dysfunction [8]. But AGEs are also formed inside cells, causing damages by generation of reactive oxygen species (ROS) [9]. They bond to the

181
182
183 Receptor of Advanced Glycation End products (RAGE) [10, 11], thus increasing
184
185 inflammation mediator release via the NF- κ B pathway [12]. Activated inflammatory and
186
187 oxidative cascades lead to the formation of new AGEs in cells. Moreover, excessive ROS
188
189 levels affect intracellular detoxification systems like the proteasome, as well as other
190
191 enzymes involved in cellular repairing. All this leads to a decrease in the antioxidative
192
193 and repair potential of cells [11]. The overall negative effects of AGEs in cells lead to
194
195 tissue and organ dysfunction [13].
196
197
198
199
200

201 The glycation process does not spare the skin. AGEs have been shown to accumulate in
202
203 the dermis and epidermis [14, 15]. Carboxymethyl-lysine (CML) and pentosidine are the
204
205 most common AGEs in the skin [15]. Aesthetic consequences due to glycation are
206
207 stiffening of the dermis leading mainly to collapsing of the skin, wrinkles formation, skin
208
209 tone yellowing and emergence of brown spots, as it can be seen in diabetic patients [16,
210
211 17]. Most compounds on the market act by preventing the binding between sugars and
212
213 proteins, or by reversing the first reversible steps of the glycation reaction. But there
214
215 are only a few compounds that can reduce the number of final AGEs accumulated in the
216
217 body [18]. Consequently, there is a growing dermatological, cosmetic and therapeutic
218
219 interest in finding compounds able to get rid of AGEs accumulated in the skin.
220
221

222 However, most of the methods reported in the literature were used to detect and
223
224 quantify glycation in food [19, 20], human urine, plasma or serum [21-24], or *in tubo*
225
226 formed AGEs by mixing a single protein with one reducing sugar [25, 26]. In the skin,
227
228 studies mainly focus on extracellular proteins modified by glycation [27, 28] and not
229
230 directly on the final AGEs formed at the end of the process. Few methods were reported
231
232 in the literature to quantify glycation in skin cells, which are suitable with the screening
233
234 of a very large number of drug candidates.
235
236
237
238
239
240

241
242
243
244
245 The goal of this work was to develop a reliable method able to detect and quantify
246
247 intracellular AGEs naturally formed and accumulated in human cells upon aging,
248
249 without using any AGE inducers. The level of AGEs was evaluated by measuring the
250
251 characteristic autofluorescence of many AGEs [21, 29] and of particular pentosidine
252
253 [30]. The developed method consist of the analysis of cell lysates using an HPLC system
254
255 coupled with a fluorescence detector, in by-pass mode to allow a direct measurement of
256
257 fluorescence using several wavelengths in the same time. The current article provides a
258
259 detailed description of the technique, and demonstrates how it can be used to screen a
260
261 large number of natural extracts in order to find new deglycation compounds capable of
262
263 reducing the intracellular glycation in human fibroblasts.
264
265
266
267
268

270 **2. Material and Methods**

272 **2.1 Chemical and reagents**

273
274 Primary normal human dermal fibroblasts (NHDF) derived from a 54-years-old woman
275
276 skin tissue were purchased from Promocell and cultured according to the supplier's
277
278 instructions in fibroblasts growth medium2 (Promocell GmbH, Heidelberg, Germany).
279
280 Glyoxal solution and phenylmethanesulfonyl fluoride (PMSF) were obtained from Sigma
281
282 (Sigma-Aldrich, Saint-Quentin Fallavier, France). Radioimmunoprecipitation assay
283
284 (RIPA) buffer and Phosphate Buffered Solution (PBS) were obtained from
285
286 ThermoFisher (ThermoFisher Scientific, Villebon sur Yvette, France). TritonX-100 was
287
288 from Euromedex (Euromedex France, Souffelweyersheim, France). Dimethyl sulfoxide
289
290 (DMSO) was obtained from Carlo Erba (Carlo Erba Reagents S.A.S, Val de Reuil, France).
291
292 Tween-20 was obtained from Acros Organics (Acros Organics, Geel, Belgium). Bovine
293
294 serum albumin (BSA) was obtained from Dutscher (Dominique Dutscher SAS, Brumath,
295
296
297
298
299
300

301
302
303 France). Paraformaldehyde was obtained from Electron Microscopy Science (EMS,
304 Hartfield, PA, U.S.A). Mouse anti-CarboxyMethyl-Lysine (CML) antibody (KH011) was
305 obtained from Cosmo Bio Co (Cosmo Bio Co LTD, Tokyo, Japan). Goat anti-mouse
306 secondary antibody Alexa-488 conjugate (A11017) was obtained from Lifetechnologies
307 (ThermoFisher Scientific, Villebon sur Yvette, France). Mounting medium with DAPI
308 was obtained from Vector (Vector Laboratories Inc, Burlingame, CA, U.S.A). MilliQ water
309 was obtained using a Millipore Synergy UV-R system (Merck-Millipore, Darmstadt,
310 Germany).
311
312
313
314
315
316
317
318
319
320
321

322 **2.1 Natural extracts**

323
324 A library of 269 ethyl acetate extracts of symbiotic microorganisms was used for this
325 study [31, 32]. Their cytotoxicity have been tested against MRC-5, MDA-MB-435 cell
326 lines. The extracts devoid of toxicity were then tested on primary dermal fibroblasts
327 (NHDF) at three concentrations (10 µg/mL, 1 µg/mL and 0,1 µg/mL in DMSO; data
328 available in Table S1 of supplementary material). The extracts having no toxic effect
329 against NHDF at 1 µg/mL were used for the screening of their activity against
330 intracellular AGEs.
331
332
333
334
335
336
337
338
339
340
341

342 **2.3 Cell culture**

343
344 Normal human dermal fibroblasts (NHDF) were grown in a humidified atmosphere of 5
345 % CO₂ at 37°C in fibroblasts growth medium².
346
347
348
349
350

351 *2.3.1 Method development*

352
353 The NHDF were seeded at the density of 7000 cells/cm² on T25 flasks at day 0.
354
355
356
357
358
359
360

361
362
363 At day 1, the culture medium was supplemented with glyoxal (final concentration: 250
364 μM and 500 μM) for 48 hours. The control cells were treated with DMSO only. On day 3,
365
366 at the end of treatment, culture medium was removed, and cells were washed with
367
368 HEPES-Buffered saline solution (4-(2-hydroxyethyl)piperazine-1-ethanesulfonic acid)
369
370 before adding fresh culture medium. Cells were cultivated for another 48 hours before
371
372 being harvested on day 5 with Trypsine-EDTA solution. Cells were counted using an
373
374 Automated Cell counter TC20 (BioRad Laboratories, Hercules, CA, U.S.A) and their
375
376 pellets were kept at -20°C until use. Experiments were done in duplicate.
377
378
379
380
381

382 383 *2.3.2 Application: Screening of natural extracts*

384
385 The NHDF were seeded at the density of 7000 cells/cm² on 24-well-plates at day 0.
386

387 At day 1, the extracts were added in the culture medium (final concentration: 1 $\mu\text{g}/\text{mL}$)
388
389 for 24 hours. Each experiment was conducted in duplicate. The control cells were
390
391 treated with DMSO only. On day 2, after 24 hours of treatment, culture medium was
392
393 removed, and cells were washed with HEPES-BSS solution before adding fresh culture
394
395 medium. Cells were cultivated for an additional 48 hours before being harvested on day
396
397 4 with a Trypsine-EDTA solution. Cells were counted, freezed and stored at -20°C until
398
399 use.
400
401
402
403

404 **2.4 Cell lysis**

405
406 Cell pellets were lysed for 30 minutes on ice, using RIPA lysis buffer in which a PMSF
407
408 solution was added to prevent the action of proteases. After centrifugation at 14000 g,
409
410 the supernatants were stored at -20°C until analysis.
411
412
413
414

415 **2.5 HPLC/Fluorescence method:**

2.5.1 Sample preparation for HPLC/fluorescence

The day of the analysis, cell lysates were diluted three times with PBS 1X, filtered, and put into an HPLC insert vial. HPLC vials were kept at 4°C within the HPLC autosampler during all the experiment.

2.5.2 HPLC/Fluorescence analysis

For the analysis of the cell lysates, a Waters 2690/S separation module HPLC system coupled with a Waters W2475 fluorescence detector was used (Waters Corporation, Guyancourt, France). Since no separation was required, a by-pass was set-up instead of the column. Wavelengths on the fluorescence detector were set at $\lambda_{\text{ex}} = 370 \text{ nm}$ / $\lambda_{\text{em}} = 445 \text{ nm}$ for measuring global AGEs amount, and at $\lambda_{\text{ex}} = 335 \text{ nm}$ / $\lambda_{\text{em}} = 385 \text{ nm}$ for measuring particular pentosidine amount, as previously described [21, 29, 30].

Mobile phase used was 100 % milliQ H₂O at a flow rate of 0.5 mL/min. Run length was 1 minute. Cell lysates (6 μL) were injected in triplicate, and a blank (water) was injected every 8 runs to confirm that no fluorescence accumulated in pipes.

2.5.3 Results analysis

Fluorescence picks were automatically integrated using Empower software (Waters Corporation, Guyancourt, France). Picks areas were analyzed and correspond to the cell lysate fluorescence value expressed in arbitrary units.

To allow the comparison between treatments, the fluorescence values were normalized for 1000 cells.

2.6 CML immunofluorescence

481
482
483 NHDF were plated on glass coverslips set into a 24-wells-plate and cultured in standard
484
485 conditions as described above. On day 4, the fibroblasts were fixed with 2 %
486
487 paraformaldehyde (500 μ L) for 12 minutes at room temperature, permeabilized with
488
489 0.2 % TritonX-100 (500 μ L) for 10 minutes and finally blocked with 5 % BSA, 0.2 %
490
491 Tween-20 (500 μ L) for further 10 minutes. Cells were then incubated with the primary
492
493 antibody anti-CML (mouse) at a concentration of 7 μ g/mL (30 μ L) at 4°C overnight,
494
495 followed by incubation with Alexa-488 anti-mouse secondary antibody diluted at 1:200
496
497 (30 μ L) for 2 hours at room temperature. After washing with 5 % BSA, 0.2 % Tween-20
498
499 (3x500 μ L), coverslips were mounted onto microscope slides using a DAPI containing
500
501 mounting medium, and observed under a confocal photonic microscope (Spinning-Disk
502
503 microscope, Roper/Nikon – parameters for DAPI: Laser 447/60 405 ; Gain : 3(4x) ;
504
505 Digitizer : 5MHz ; EM gain : 150 ; Exposition : 200 ms ; Laser power : 30% - parameters
506
507 for Alexa 488 : Laser 525/45 491 ; Gain : 3 (4x) ; Digitizer : 5MHz ; EM gain : 200 ;
508
509 Exposition : 300ms ; Laser power: 25%). Images are recorded using a Z stack, allowing
510
511 fluorescence to be recorded at different positions in the cell. Five images were recorded
512
513 by coverslips (ten pictures per treatment condition). All pictures were taken with the
514
515 same microscope parameters. Fluorescence quantification on the images was done
516
517 using ImageJ software.
518
519
520
521
522
523

524 **2.7 Statistical analysis**

525
526 Data were presented as mean \pm standard error of the mean. The mean data were
527
528 analyzed with one-way analysis of variance (one way ANOVA) followed by Dunnett's
529
530 multiple comparison test. A $P < 0.05$ was considered to be significant.
531
532
533
534

535 **2.8 Method validation**

541
542
543 To determine the reproducibility of the method, we calculated the relative standard
544 deviation (RSD) for triplicates of the same sample, and biological duplicates of the same
545 treatment (data available in Table S2 of supplementary material).
546
547
548
549
550

551 552 **3. Results**

553 *3.1 Method development*

554
555 We first examined whether the proposed approach was able to detect and quantify the
556 variations in the amount of AGEs and pentosidine in lysates of fibroblasts treated with
557 250 μ M and 500 μ M of glyoxal for 48 hours.
558
559
560

561 Glyoxal is a dicarbonyl formed *in vivo* mainly by auto-oxidation of reducing sugars and
562 by lipid peroxidation. Both highly reactive carbonyl groups of glyoxal react with the
563 amino groups of proteins to form AGEs as previously reported [33-35].
564
565
566

567 Lysates of glyoxal treated cells and lysates of untreated controls were injected in
568 triplicate in the HPLC system in by-pass mode, using MilliQ H₂O as mobile phase, and
569 the signal was recorded with a fluorescence detector using two sets of wavelengths for
570 the simultaneous detection of AGEs ($\lambda_{\text{ex}} = 370 \text{ nm} / \lambda_{\text{em}} = 445 \text{ nm}$) and pentosidine (λ_{ex}
571 $= 335 \text{ nm} / \lambda_{\text{em}} = 385 \text{ nm}$). The use of the HPLC system allows the analysis of small
572 amounts of samples, with good reproducibility. The fluorescence spectra of pentosidine
573 recorded in control cells lysate (triplicate) are presented in Figure 2. The fluorescence
574 value corresponds to peak integration value. To allow a reliable comparison between
575 the treatments, the number of cells harvested at the end of the cell culture was counted,
576 and the fluorescence values were normalized for 1000 cells.
577
578
579
580
581
582
583
584
585
586
587
588
589
590

591
592
593 As shown in Table I, the treatment of fibroblasts with glyoxal increases significantly the
594 fluorescence detected in cell lysates for both AGEs and pentosidine, in a dose-dependent
595
596
597
598
599
600

601
602
603 manner. A 1.3-fold and 2.2-fold increase in the amount of intracellular AGEs present in
604
605 cells treated respectively with 250 μ M and 500 μ M of glyoxal for 48 hours, compared to
606
607 controls was observed. For pentosidine, a 1.4-fold and 2.6-fold increase in cells treated
608
609 respectively with 250 μ M and 500 μ M of glyoxal was detected.
610

611
612 To valid these findings, we analyzed the level of carboxymethyl-lysine (CML) by
613
614 immunocytochemistry in cells treated with 500 μ M of glyoxal for 48 hours (Fig. 3.). CML
615
616 is an AGE forming adducts on proteins. Quantification of the immunofluorescence signal
617
618 on images taken by confocal photonic microscopy shows that the intracellular CML
619
620 content was indeed significantly higher in cells treated with glyoxal (1.57 ± 0.07
621
622 increase compared to non-treated control cells).
623
624
625
626

627 *3.2 Application: The effect of natural products on the amount of intracellular* 628 629 *pentosidine* 630

631
632 As the developed method was able to detect variations in the content of AGEs in cells
633
634 treated with different concentrations of glyoxal, we used it to screen eighty natural
635
636 extracts and evaluate their potential to reduce the quantity of intracellular AGEs and
637
638 pentosidine in human skin cells. Treatment of fibroblasts with extracts was done for 24
639
640 hours, in biological duplicate. The intracellular AGEs and pentosidine level was
641
642 recorded by HPLC with fluorescence detector as described above. Aminoguanidine, an
643
644 AGE inhibitor compound, was chosen as control. Table II show the results of twenty-
645
646 three of the extracts as the mean amount of pentosidine in cells compared to control.
647
648
649
650

651
652 The screening conducted in biological duplicates showed that aminoguanidine did not
653
654 reduce the intracellular amount of pentosidine. However, among the eighty natural
655
656 extracts, seven of them were shown to significantly reduce the intracellular content of
657
658
659
660

661
662
663 pentosidine in dermal fibroblasts. SNB-GTC2701 was the most active extract, reducing
664
665 intracellular pentosidine content by 32 % in fibroblasts after 24 hours of treatment at 1
666
667 $\mu\text{g/mL}$.
668
669
670

671 672 *3.3 Reproducibility* 673

674 The reproducibility of the method was evaluated taking into account the triplicates of
675
676 the same sample and biological duplicates of the same treatment.
677

678 The relative standard deviations of samples (RSD) between the triplicates of the same
679
680 sample ranged within 10 % (except for treatment SNB-CN76) for AGEs and for
681
682 pentosidine (Table S2). RSD calculated between biological duplicates showed good
683
684 reproducibility as well (< 10 %). According to these results, the method can be
685
686 considered as robust.
687
688
689
690

691 **4. Discussion** 692

693
694 The present method was developed to quantify the amount of intracellular AGEs and
695
696 pentosidine in human dermal fibroblasts lysates, using their characteristic
697
698 autofluorescent properties.
699

700 To develop the method, we used glyoxal treated fibroblasts. Glyoxal is mainly produced
701
702 during the autooxidation of reducing sugars, and is a source of macromolecular damage
703
704 in cells. Treatment of fibroblasts with glyoxal was shown to induce a senescent
705
706 phenotype *in vitro*, and to lead to an increase of AGEs levels, thus providing a model of
707
708 accelerated cellular aging [33].
709

710
711 Results obtained with the developed method confirmed that glyoxal induces a change in
712
713 the AGE content in fibroblasts. Moreover, the HPLC-fluorescent method was efficient to
714
715 detect and quantify these changes.
716
717
718
719
720

721
722
723 Besides, by analyzing the results obtained during the development phase, we noticed
724 that the glycation level of the non-treated dermal fibroblasts obtained from a 54 years
725 old donor was high enough to be easily detected and quantified by the HPLC coupled
726 with fluorescence method. In fact, AGEs accumulates *in vivo* during normal aging, and
727 the detection of naturally occurring AGEs in fibroblasts with our method was of high
728 interest for the next step of our project. This allowed us to screen the natural extracts
729 library on cells that have not undergone glyoxal treatment, thus enabling the screening
730 to be performed under conditions closest to the biological conditions *in vivo*.
731

732
733 During the screening, aminoguanidine was chosen as a control compound. This
734 molecule works as a scavenger of reactive dicarbonyl intermediates in the Maillard
735 reaction, therefore inhibiting AGE formation. Our results showed that aminoguanidine
736 did not reduce the pentosidine level in fibroblasts. This finding is in line with published
737 data on its mode of action preventing the condensation of reducing sugars with amino-
738 acids residues, or inhibiting the first reversible reaction of the glycation process [36].
739 We provide new evidence that aminoguanidine is not able to target AGEs at their final
740 stage.
741

742
743 Among eighty natural extracts tested, seven of them showed positive results on
744 pentosidine, significantly reducing its content in dermal fibroblasts after 24 hours of
745 treatment. Comparing these results with those of aminoguanidine, we hypothesize that
746 the mechanism of action of the tested active extracts might be linked to a possible
747 activation or inhibition of specific biological pathways. Literature shows that AGE
748 receptor (AGER) subunit AGER-1 (OST-48) binds to AGEs, triggering endocytosis and
749 elimination of AGEs by cells, while this receptor does not bind to early glycation
750 products like Amadori products [37-39]. Pentosidine can be degraded through this
751 mechanism. We observed by western blot using a specific AGER-1 antibody that AGER-1
752
753
754
755
756
757
758
759
760
761
762
763
764
765
766
767
768
769
770
771
772
773
774
775
776
777
778
779
780

781
782
783 was overexpressed in cells treated with three of the active extracts (Figure S1).
784

785 Although further investigations will be necessary, it is possible that the active extracts
786 trigger a natural cell detoxification mechanism.
787

788
789 Due to the dermatological interest of finding compounds able to decrease the amount of
790 formed AGEs in skin, an effort was made to make the assay more rapid and as simple as
791 possible, allowing the screening of a large number of candidates in one time.
792
793

794 The screening of a large number of substances in a biological test requires cultivating
795 cells in large amounts. But miniaturization of biological tests into multiwell plates lower
796 the available quantity of samples to be analyzed. The main advantage of using an HPLC
797 system is to benefit from the auto sampler allowing precise sampling of small amounts
798 like few μL . This allowed us to miniaturize our biological screening into 24-wells plates,
799 and so to decrease the amount of cells to be cultivated as well as the extract quantity to
800 be applied as treatment.
801
802
803
804
805
806
807
808
809
810

811 812 813 **5. Conclusion** 814

815
816 The method described in this article allows detecting and quantifying intracellular
817 levels of AGEs in human dermal fibroblasts. It is reliable, reproducible, simple and can
818 be performed at rather low-cost. The use of HPLC coupled to fluorescence detection has
819 many advantages. First, the fluorescence detection at two wavelengths at the same time
820 reduces the quantity of sample required for analysis (6 μL per injections), allowing
821 culture of cells in 24-wells plates. Then, once the cells harvested, one requires only a
822 few steps of sample preparation. Finally, the automatic injection of the samples in a
823 short one-minute run, with good reproducibility between technical and biological
824 replicates, makes it suitable for the rapid and reliable screening of a large number of
825 samples.
826
827
828
829
830
831
832
833
834
835
836
837
838
839
840

841
842
843 Contrary to commonly used methods i.e. *in tubo* tests employing one reducing sugar
844
845 and one protein or methods targeting extracellular proteins modified by glycation, our
846
847 experimental approach allows detection and quantification of intracellular AGEs formed
848
849 and accumulated during aging in cells without induction of glycation.
850

851
852 Eventually, the method was applied to test natural extracts and revealed the potential of
853
854 some of them to reduce the amount of AGEs naturally accumulated in cells with aging,
855
856 thus suggesting that new deglycation compounds of dermatological and cosmetic
857
858 interest may be discovered. The mode of action of the active extracts needs to be further
859
860 characterized but seems to involve complex biological reactions. Thus, the molecules
861
862 responsible for the activity will be characterized after bioguided isolation.
863
864
865
866
867
868

869 **Aknowledgements**

870
871 The present work has benefited from the facilities and expertise of the HPLC facilities of
872
873 CNRS-ICSN. We shall address our appreciation to Odile Thoison and Frank Pelissier for
874
875 their technical assistance.
876

877
878 The present work has benefited from the facilities and expertise of the light microscopy
879
880 facilities of Imagerie-Gif. This core facility is member of the Infrastructures en Biologie
881
882 Santé et Agronomie (IBiSA), and is supported by the French National Research Agency
883
884 under Investments for the Future programs “France-BioImaging”, and the Labex “Saclay
885
886 Plant Science” (ANR-10-INSB-04-01 and ANR-11-IDEX-0003-02, respectively). A special
887
888 thanks to Romain Le Bars and Laëtitia Besse for their invaluable help during the
889
890 microscopy sessions.
891
892
893
894
895
896
897
898
899
900

Funding

This work has benefited from a CIFRE grant managed by the Association Nationale de la Recherche et de la Technologie, France (ANRT, n°2013-1326), and from an “Investissement d'Avenir” grant managed by Agence Nationale de la Recherche, France (CEBA, ref. ANR-10-LABX-25-01).

Conflict of Interest

The authors declare that they have no conflict of interest.

REFERENCES

1. Maillard, L. Action des acides aminés sur les sucres, formation des mélanoidines par voie méthodique. *C R Acad Sci.* (154):66-8 (1912).
2. Ahmed, N. Advanced glycation endproducts—role in pathology of diabetic complications. *Diabetes Res Clin Prat.* 67(1):3-21 (2005).
3. Vlassara, H. Advanced glycation in health and disease: role of the modern environment. *Ann N Y Acad Sci.* 1043:452-60 (2005).
4. Kasper, M. and Funk, R.H. Age-related changes in cells and tissues due to advanced glycation end products (AGEs). *Arch Gerontol Geriatr.* 32(3):233-43 (2001).
5. Goldin, A., Beckman, J.A., Schmidt, A.M. and Creager, M.A. Advanced glycation end products: sparking the development of diabetic vascular injury. *Circulation.* 114(6):597-605 (2006).
6. Kume, S., Takeya, M., Mori, T., Araki, N., Suzuki, H., Horiuchi, S., et al. Immunohistochemical and ultrastructural detection of advanced glycation end products in atherosclerotic lesions of human aorta with a novel specific monoclonal antibody. *Am J Pathol.* 147(3):654-67 (1995).
7. Baynes, J.W. The role of AGEs in aging: causation or correlation. *Exp Gerontol.* 36(9):1527-37 (2001).
8. Paul, R.G. and Bailey, A.J. The effect of advanced glycation end-product formation upon cell-matrix interactions. *Int J Biochem Cell Biol.* 31(6):653-60 (1999).
9. Valencia, J.V., Weldon, S.C., Quinn, D., Kiers, G.H., DeGroot, J., TeKoppele, J.M., et al. Advanced glycation end product ligands for the receptor for advanced glycation end products: biochemical characterization and formation kinetics. *Anal Biochem.* 324(1):68-78 (2004).
10. Liu, Y., Liang, C., Liu, X., Liao, B., Pan, X., Ren, Y., et al. AGEs increased migration and inflammatory responses of adventitial fibroblasts via RAGE, MAPK and NF-kappaB pathways. *Atherosclerosis.* 208(1):34-42 (2010).
11. Ott, C., Jacobs, K., Haucke, E., Navarrete Santos, A., Grune, T. and Simm, A. Role of advanced glycation end products in cellular signaling. *Redox Biol.* 2:411-29 (2014).
12. Kasper, M., Schinzel, R., Niwa, T., Munch, G., Witt, M., Fehrenbach, H., et al. Experimental induction of AGEs in fetal L132 lung cells changes the level of intracellular cathepsin D. *Biochem Biophys Res Commun.* 261(1):175-82 (1999).
13. Badenhorst, D., Maseko, M., Tsoetsi, O.J., Naidoo, A., Brooksbank, R., Norton, G.R., et al. Cross-linking influences the impact of quantitative changes in myocardial collagen on cardiac stiffness and remodelling in hypertension in rats. *Cardiovasc Res.* 57(3):632-41 (2003).
14. Kawabata, K., Yoshikawa, H., Saruwatari, K., Akazawa, Y., Inoue, T., Kuze, T., et al. The presence of N(epsilon)-(Carboxymethyl) lysine in the human epidermis. *Biochim Biophys Acta.* 1814(10):1246-52 (2011).

- 961
962
963
964
965
966
967
968
969
970
971
972
973
974
975
976
977
978
979
980
981
982
983
984
985
986
987
988
989
990
991
992
993
994
995
996
997
998
999
1000
1001
1002
1003
1004
1005
1006
1007
1008
1009
1010
1011
1012
1013
1014
1015
1016
1017
1018
1019
1020
15. Gkogkolou, P. and Bohm, M. Advanced glycation end products: Key players in skin aging? *Dermatoendocrinol.* 4(3):259-70 (2012).
 16. Lee, E.J., Kim, J.Y. and Oh, S.H. Advanced glycation end products (AGEs) promote melanogenesis through receptor for AGEs. *Sci Rep.* 6:27848 (2016).
 17. Dyer, D.G., Dunn, J.A., Thorpe, S.R., Bailie, K.E., Lyons, T.J., McCance, D.R., et al. Accumulation of Maillard reaction products in skin collagen in diabetes and aging. *J Clin Invest.* 91(6):2463-9 (1993).
 18. Yang, S., Litchfield, J.E. and Baynes, J.W. AGE-breakers cleave model compounds, but do not break Maillard crosslinks in skin and tail collagen from diabetic rats. *Arch Biochem Biophys.* 412(1):42-6 (2003).
 19. Tareke, E., Forslund, A., Lindh, C.H., Fahlgren, C. and Ostman, E. Isotope dilution ESI-LC-MS/MS for quantification of free and total Nepsilon-(1-Carboxymethyl)-L-Lysine and free Nepsilon-(1-Carboxyethyl)-L-Lysine: comparison of total Nepsilon-(1-Carboxymethyl)-L-Lysine levels measured with new method to ELISA assay in gruel samples. *Food Chem.* 141(4):4253-9 (2013).
 20. He, J., Zeng, M., Zheng, Z., He, Z. and Chen, J. Simultaneous determination of Nε-(carboxymethyl) lysine and Nε-(carboxyethyl) lysine in cereal foods by LC-MS/MS. *Eur Food Res Technol.* (238):367-74 (2014).
 21. Munch, G., Keis, R., Wessels, A., Riederer, P., Bahner, U., Heidland, A., et al. Determination of advanced glycation end products in serum by fluorescence spectroscopy and competitive ELISA. *Eur J Clin Chem Clin Biochem.* 35(9):669-77 (1997).
 22. Hanssen, N.M., Engelen, L., Ferreira, I., Scheijen, J.L., Huijberts, M.S., van Greevenbroek, M.M., et al. Plasma levels of advanced glycation endproducts Nepsilon-(carboxymethyl)lysine, Nepsilon-(carboxyethyl)lysine, and pentosidine are not independently associated with cardiovascular disease in individuals with or without type 2 diabetes: the Hoorn and CODAM studies. *J Clin Endocrinol Metab.* 98(8):E1369-73 (2013).
 23. Price, D.L., Rhett, P.M., Thorpe, S.R. and Baynes, J.W. Chelating activity of advanced glycation end-product inhibitors. *J Biol Chem.* 276(52):48967-72 (2001).
 24. De La Maza, M.P., Bravo, A., Leiva, L., GattÁS, V., Petermann, M., Garrido, F., et al. Fluorescent serum and urinary advanced glycooxidation end-products in non-diabetic subjects. *Biological Research.* 40:203-12 (2007).
 25. Ahmed, N., Argirov, O.K., Minhas, H.S., Cordeiro, C.A. and Thornalley, P.J. Assay of advanced glycation endproducts (AGEs): surveying AGEs by chromatographic assay with derivatization by 6-aminoquinolyl-N-hydroxysuccinimidyl-carbamate and application to Nepsilon-carboxymethyl-lysine- and Nepsilon-(1-carboxyethyl)lysine-modified albumin. *Biochem J.* 364(1):1-14 (2002).
 26. Schmitt, A., Schmitt, J., Munch, G. and Gasic-Milencovic, J. Characterization of advanced glycation end products for biochemical studies: side chain modifications and fluorescence characteristics. *Anal Biochem.* 338(2):201-15 (2005).
 27. Gasser, P., Arnold, F., Peno-Mazzarino, L., Bouzoud, D., Luu, M.T., Lati, E., et al. Glycation induction and antiglycation activity of skin care ingredients on living human skin explants. *Int J Cosmet Sci.* 33(4):366-70 (2011).
 28. Kobayashi, K. and Igimi, H. Glycation index of hair for non-invasive estimation of diabetic control. *Biol Pharm Bull.* 19(4):487-90 (1996).
 29. Galler, A., Muller, G., Schinzel, R., Kratzsch, J., Kiess, W. and Munch, G. Impact of metabolic control and serum lipids on the concentration of advanced glycation end products in the serum of children and adolescents with type 1 diabetes, as determined by fluorescence spectroscopy and nepsilon-(carboxymethyl)lysine ELISA. *Diabetes Care.* 26(9):2609-15 (2003).
 30. Odetti, P., Fogarty, J., Sell, D.R. and Monnier, V.M. Chromatographic quantitation of plasma and erythrocyte pentosidine in diabetic and uremic subjects. *Diabetes.* 41(2):153-9 (1992).
 31. Casella, T.M., Eparvier, V., Mandavid, H., Bendelac, A., Odonne, G., Dayan, L., et al. Antimicrobial and cytotoxic secondary metabolites from tropical leaf endophytes: Isolation of antibacterial agent pyrrocidine C from *Lewia infectoria* SNB-GTC2402. *Phytochemistry.* 96:370-7 (2013).
 32. Nirma, C., Eparvier, V. and Stien, D. Antifungal Agents from *Pseudallescheria boydii* SNB-CN73 Isolated from a *Nasutitermes* sp. Termite. *J Nat Prod.* 76(5):988-91 (2013).
 33. Sejersen, H. and Rattan, S.I. Dicarbonyl-induced accelerated aging in vitro in human skin fibroblasts. *Biogerontology.* 10(2):203-11 (2009).
 34. Bulteau, A.L., Verbeke, P., Petropoulos, I., Chaffotte, A.F. and Friguet, B. Proteasome inhibition in glyoxal-treated fibroblasts and resistance of glycated glucose-6-phosphate dehydrogenase to 20 S proteasome degradation in vitro. *J Biol Chem.* 276(49):45662-8 (2001).

- 1021
1022
1023 35. Ahmed, M.U., Brinkmann Frye, E., Degenhardt, T.P., Thorpe, S.R. and Baynes, J.W. N-epsilon-
1024 (carboxyethyl)lysine, a product of the chemical modification of proteins by methylglyoxal, increases with
1025 age in human lens proteins. *Biochem J.* 324(2):565-70 (1997).
1026 36. Nagai, R., Murray, D.B., Metz, T.O. and Baynes, J.W. Chelation: A Fundamental Mechanism of
1027 Action of AGE Inhibitors, AGE Breakers, and Other Inhibitors of Diabetes Complications. *Diabetes.*
1028 61(3):549-59 (2012).
1029 37. Li, Y.M., Mitsuhashi, T., Wojciechowicz, D., Shimizu, N., Li, J., Stitt, A., et al. Molecular identity and
1030 cellular distribution of advanced glycation endproduct receptors: relationship of p60 to OST-48 and p90
1031 to 80K-H membrane proteins. *Proc Natl Acad Sci U S A.* 93(20):11047-52 (1996).
1032 38. Lu, C., He, J.C., Cai, W., Liu, H., Zhu, L. and Vlassara, H. Advanced glycation endproduct (AGE)
1033 receptor 1 is a negative regulator of the inflammatory response to AGE in mesangial cells. *Proc Natl Acad*
1034 *Sci U S A.* 101(32):11767-72 (2004).
1035 39. Yang, Z., Makita, Z., Horii, Y., Brunelle, S., Cerami, A., Sehajpal, P., et al. Two novel rat liver
1036 membrane proteins that bind advanced glycosylation endproducts: relationship to macrophage receptor
1037 for glucose-modified proteins. *J Exp Med.* 174(3):515 (1991).
1038
1039
1040
1041
1042
1043
1044
1045
1046
1047
1048
1049
1050
1051
1052
1053
1054
1055
1056
1057
1058
1059
1060
1061
1062
1063
1064
1065
1066
1067
1068
1069
1070
1071
1072
1073
1074
1075
1076
1077
1078
1079
1080

1081
1082
1083 Legends to figures:
1084

1085 **Figure 1:** Glycation reaction of proteins with glucose leading to the formation of AGEs,
1086 and structure of Pentosidine crosslink.
1087

1088
1089 **Figure 2:** Example of fluorescence signal recorded for pentosidine ($\lambda_{ex} = 335 \text{ nm} / \lambda_{em} =$
1090 385 nm) in lysate of control cells. Injections were done in triplicate. Peak integration
1091 (area) was done with Empower software (Waters).
1092
1093

1094 **Figure 3:** Confocal microscopy images (X40) of human dermal fibroblasts treated for 48
1095 hours with (a) DMSO as control and (b) 500 μM of glyoxal. Nucleus labeling by DAPI
1096 (blue) ; Immunological labeling of CML by Alexa 488 (green).
1097
1098
1099
1100
1101
1102
1103
1104
1105
1106

1107 Tables:
1108

1109 **Table I.** AGEs ($\lambda_{ex} = 370 \text{ nm} / \lambda_{em} = 445 \text{ nm}$) and pentosidine expression ($\lambda_{ex} = 335 \text{ nm} /$
1110 $\lambda_{em} = 385 \text{ nm}$) in NHDF treated with 250 μM and 500 μM glyoxal for 48 hours.
1111
1112 Concentrations have been normalized relatively to the negative control, for 1000 cells.
1113
1114 Significance levels when compared to negative control were calculated by one-way
1115 ANOVA followed by Dunett's multiple comparison test *** $P < 0.001$ compared to control.
1116
1117
1118
1119
1120
1121

1122

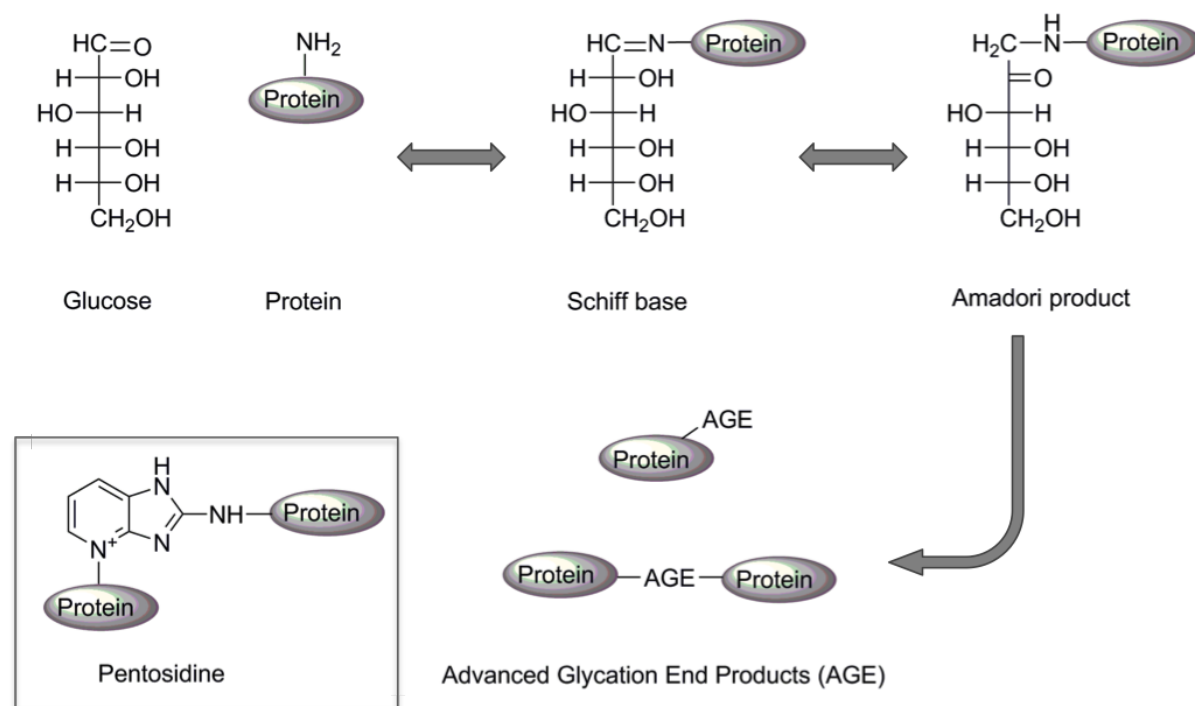
Treatment	AGEs expression \pm SD	Pentosidine \pm SD
GO 250 μM	1.32 \pm 0.16 ***	1.38 \pm 0.03 ***
GO 500 μM	2.16 \pm 0.07 ***	2.61 \pm 0.02 ***

1123
1124
1125
1126
1127
1128
1129

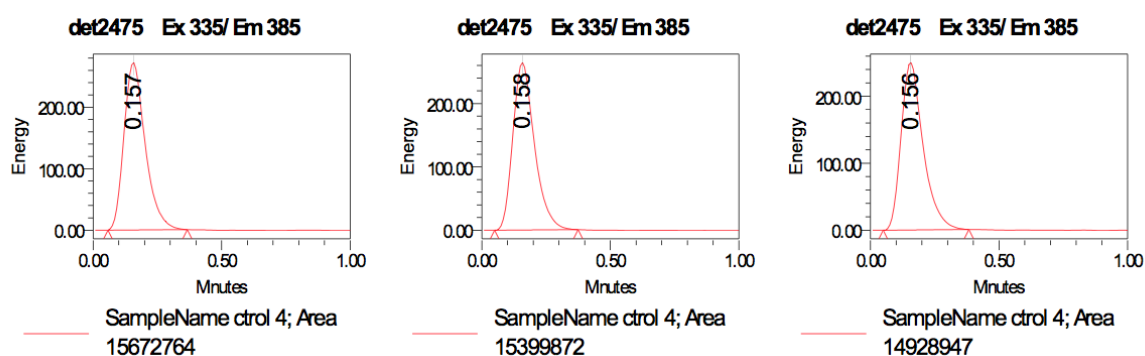
1141
 1142
 1143
 1144
 1145
 1146 **Table II.** Effect of 23 different microbial extracts and aminoguanidine on pentosidine
 1147
 1148 expression compared to control, measured by the HPLC/fluorescence method in human
 1149
 1150 dermal fibroblasts. Concentrations have been normalized relatively to the negative
 1151
 1152 control, for 1000 cells. Significance levels when compared to negative control were
 1153
 1154 calculated by one-way ANOVA followed by Dunett's multiple comparison test; *P < 0.05;
 1155
 1156 **P < 0.01; ***P < 0.001 compared to control, ns = not significant.
 1157
 1158
 1159
 1160

Treatment	Pentosidine amount \pm SD
Control (untreated)	1.00 \pm 0.05
Aminoguanidine	1.13 \pm 0.18 ^{ns}
SNB-GTC2701	0.68 \pm 0.07 ^{***}
SNB-CN20	0.71 \pm 0.01 ^{**}
SNB-CN102	0.76 \pm 0.03 ^{**}
SNB-CN55	0.79 \pm 0.01 ^{**}
SNB-CN76	0.80 \pm 0.03 ^{***}
SNB-GSS07	0.85 \pm 0.04 ^{ns}
SNB-CN54	0.87 \pm 0.05 [*]
SNB-CN79	0.87 \pm 0.07 ^{ns}
SNB-GSS04	0.88 \pm 0.01 ^{**}
SNB-CN13	0.89 \pm 0.09 ^{ns}
SNB-CN59	0.89 \pm 0.04 ^{ns}
SNB-GTC2810	0.91 \pm 0.10 ^{ns}
SNB-CN104	0.93 \pm 0.04 ^{ns}
SNB-CN66	0.93 \pm 0.01 ^{ns}
SNB-CN27	0.94 \pm 0.10 ^{ns}
SNB-CN69	0.97 \pm 0.11 ^{ns}
SNB-CN67	0.97 \pm 0.05 ^{ns}
SNB-CN75	0.98 \pm 0.05 ^{ns}
SNB-LD 9.2	1.02 \pm 0.10 ^{ns}
SNB-CN98	1.14 \pm 0.03 ^{ns}
SNB-CN1	1.16 \pm 0.09 [*]
SNB-CN85	1.18 \pm 0.04 ^{ns}
SNB-CN10	1.58 \pm 0.27 ^{**}

1201
1202
1203
1204
1205
1206 **Figures:**
1207



1229
1230 **Figure 1.** Glycation reaction of proteins with glucose leading to the formation of AGEs,
1231 and structure of Pentosidine crosslink.
1232
1233
1234
1235
1236
1237



1250 **Figure 2.** Example of fluorescence signal recorded for pentosidine ($\lambda_{ex} = 335 \text{ nm} / \lambda_{em} =$
1251 385 nm) in lysate of control cells. Injections were done in triplicate. Peak integration
1252 (area) was done with Empower software (Waters).
1253
1254
1255
1256
1257
1258
1259
1260

1261
1262
1263
1264
1265
1266
1267
1268
1269
1270
1271
1272
1273
1274
1275
1276
1277
1278
1279
1280
1281
1282
1283
1284
1285
1286
1287
1288
1289
1290
1291
1292
1293
1294
1295
1296
1297
1298
1299
1300
1301
1302
1303
1304
1305
1306
1307
1308
1309
1310
1311
1312
1313
1314
1315
1316
1317
1318
1319
1320

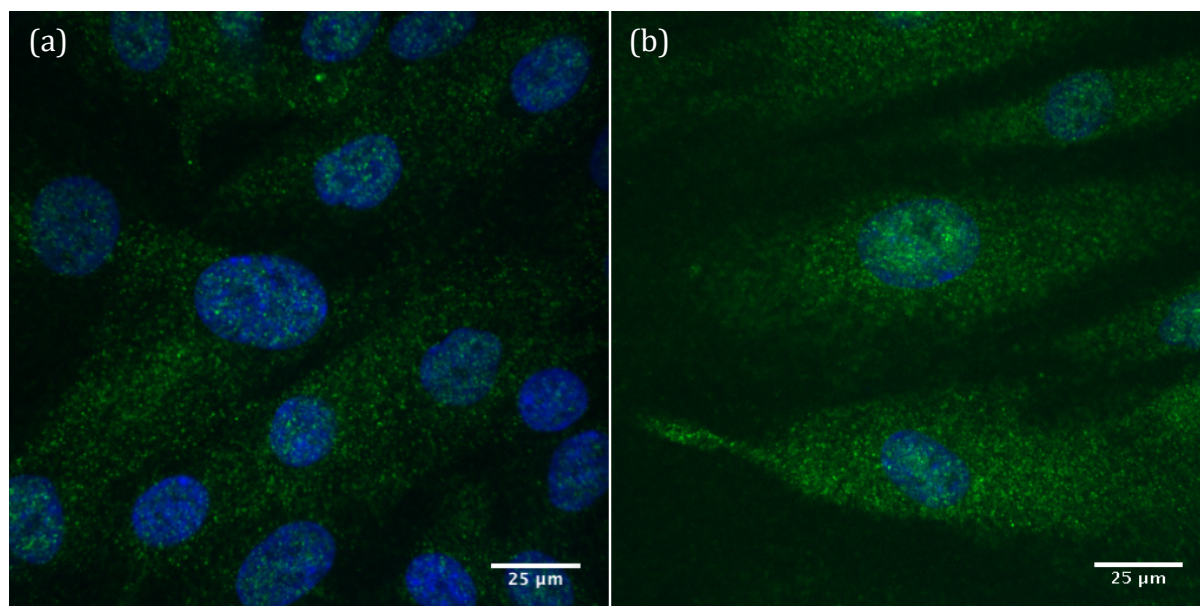


Figure 3. Confocal microscopy images (X40) of human dermal fibroblasts treated for 48 hours with (a) DMSO as control and (b) 500 μM of glyoxal. Nucleus labeling by DAPI (blue) ; Immunological labeling of CML by Alexa 488 (green).

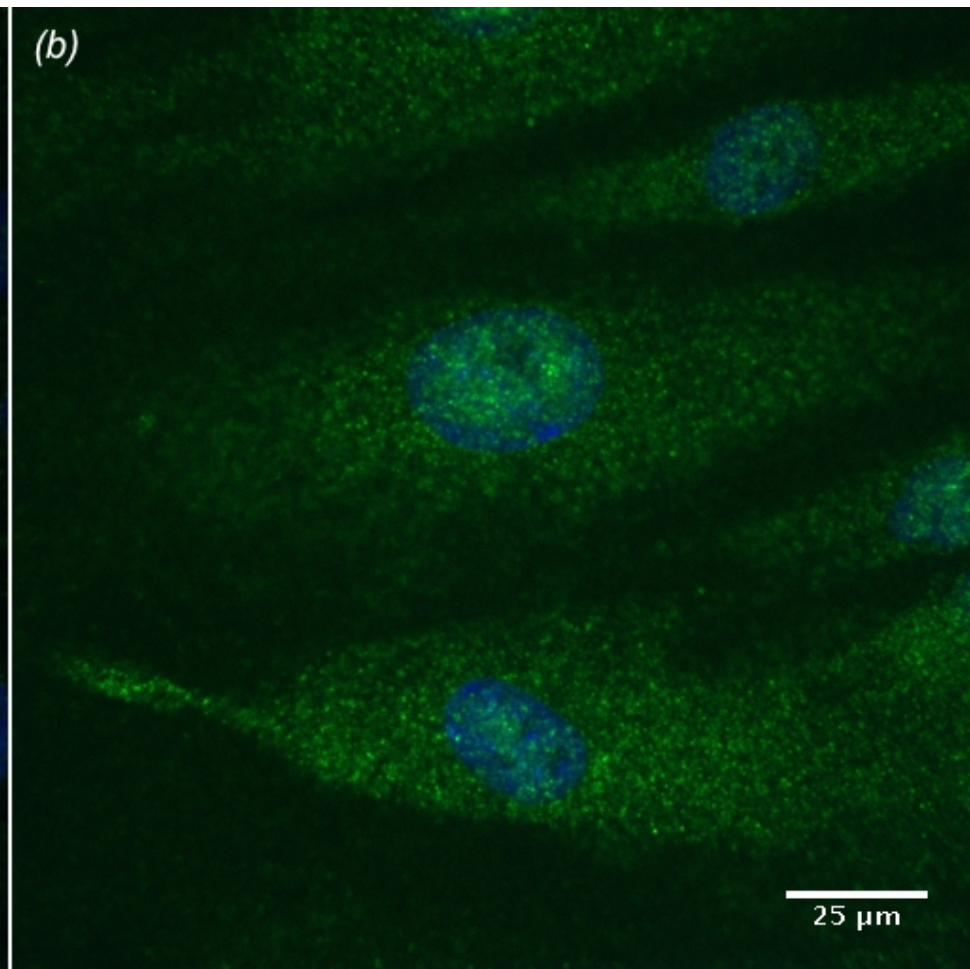
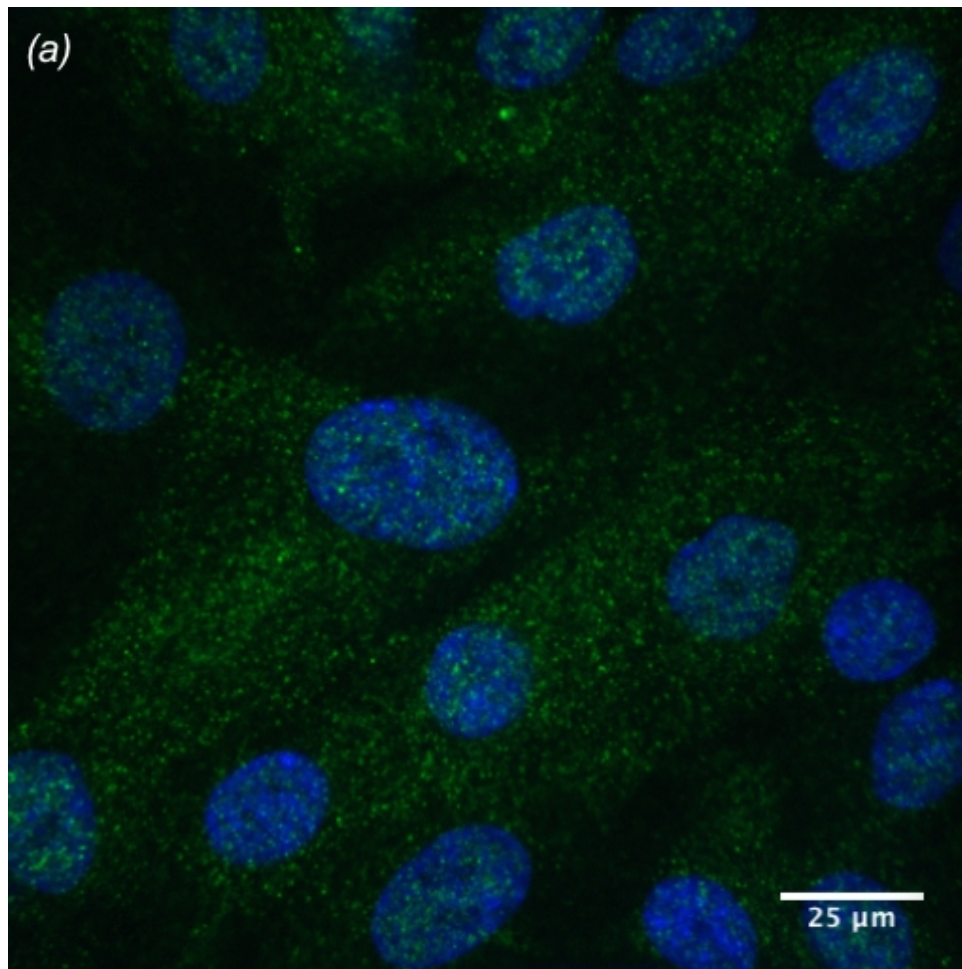


Table S1. Viability of NHDF treated for 24 heures with ethyl acetate natural extracts at 10 µg/mL, 1 µg/mL and 0,1 µg/mL in DMSO.

Extracts SNB n°	% Viability at 10 µg/mL	% Viability at 1 µg/mL	% Viability at 0,1 µg/mL	Extracts SNB n°	% Viability at 10 µg/mL	% Viability at 1 µg/mL	% Viability at 0,1 µg/mL
CN1	10,3	65,1	94,4	CN111	11,3	95,6	91,4
CN10	10,5	62,1	90,1	CN112	9,9	89,0	91,5
CN100	79,4	92,8	98,3	CN16	89,1	94,0	90,8
CN11	10,6	58,5	86,2	CN17	88,6	92,3	90,4
CN13	54,5	91,0	94,8	CN29	44,9	86,8	85,4
CN14	10,6	55,9	91,6	CN37B	106,6	92,4	92,9
CN15	<5,0	91,0	92,7	CN55	9,6	86,4	93,4
CN2	10,7	92,1	94,2	CN56	18,4	94,2	94,1
CN20	10,1	86,6	93,2	CN57	11,1	79,7	91,9
CN27	98,4	93,0	92,6	CN60	28,2	97,8	96,7
CN28	98,3	97,4	91,3	CN60bis	9,9	90,0	89,6
CN3	10,5	59,1	90,2	CN65	19,3	89,4	88,7
CN4	13,1	90,5	88,9	CN70	<5,0	ND	87,0
CN52	112,2	91,6	89,3	CN36A	129,7	ND	89,0
CN61	96,7	88,7	89,1	CN71	11,1	120,0	102,3
CN69	15,2	86,6	90,4	CN72	10,0	115,6	92,9
CN78	49,5	93,3	89,2	CN73	50,6	107,1	93,9
CN8	73,1	93,8	90,3	CN74	14,0	97,5	95,4
CN88	71,6	88,4	89,9	CN 82	80,3	92,7	92,9
CN89	<5,0	92,7	92,5	CN84	16,9	87,4	88,4
CN90	72,9	92,0	93,8	CN85	34,9	83,5	84,1
CN91	92,0	97,3	91,3	CN87	11,9	83,6	90,8
CN92	13,4	94,4	96,2	GSS11	28,1	85,0	87,2
CN94	101,1	96,1	92,3	GSS15	49,5	89,2	83,8
CN95	102,8	96,4	92,2	GTC0202	12,7	88,2	88,5
CN96	9,7	97,3	91,5	GTC2401	21,5	88,5	88,4
CN97	23,6	99,9	100,2	GTC2701	18,3	89,8	87,3
CN98	64,9	90,2	88,9	GTC2809	10,1	93,8	93,3
CN99	100,0	91,2	88,2	CN75	10,8	91,9	101,2
CN102	9,8	90,2	90,5	CN76	98,3	101,3	97,8
CN103	9,9	89,4	91,3	GTC2810	28,7	85,7	91,3
CN104	100,5	90,4	87,1	GTC2822	23,9	89,0	91,2
CN109	10,3	93,7	91,8	GTC3002	63,4	92,4	92,5
CN110	15,2	92,4	88,7	GSS07	11,0	91,7	91,6
LD2.10.2	51,9	84,5	97,7	GSS04	49,9	91,8	86,8
LD2.13	16,1	89,5	87,5	LD8.9	30,0	96,0	96,0
LD3.4	30,1	89,3	94,6	CN67	84,7	95,1	93,3
LD6.5.2	17,4	87,5	98,6	CN68	<5,0	ND	ND
LD7.1	9,9	91,6	98,3	Levure rose	<5,0	74,4	77,9

LD8.6	9,8	102,4	108,2	CN113	10,1	79,5	81,6
CN79	100,9	82,5	85,3	CN64	10,1	92,9	89,0
LD9.2	<5,0	88,7	89,1	CN66	98,6	90,0	92,3
CN59	12,7	86,5	92,4	CN54	90,4	89,9	90,2
CN62	39,2	93,6	88,0				

ND = Not determined.

Table S2. Reproducibility expressed as Relative Standard Deviation (RSD) between triplicates of the same sample, and between biological duplicates of the same treatment.

Reproducibility between triplicates			Reproducibility: between biological duplicates		
Extracts SNB n°	RSD for AGEs measurement (%)	RSD for Pentosidine measurement (%)	Extracts SNB n°	RSD for AGEs measurement (%)	RSD for Pentosidine measurement (%)
Control	4.0	2.4	Control	12.0	2.9
CN59	4.7	2.2	CN59	3.9	1.5
CN79	3.7	3.8	CN79	3.7	4.2
CN76	15.3	6.5	CN76	16.5	6.1
GSS04	4.5	4.6	GSS04	3.5	3.1
CN75	2.8	0.2	CN75	4.4	0.1
CN67	5.5	2.8	CN67	5.6	2.4
LD 9.2	4.1	19.3	LD 9.2	6.4	16.4
GSS07	1.5	0.7	GSS07	2.4	4.4
CN66	2.0	3.4	CN66	4.1	3.1
CN85	11.8	0.4	CN85	7.5	3.3
CN55	2.7	1.5	CN55	10.7	9.0
CN1	2.4	1.6	CN1	1.8	1.3
CN102	7.9	2.6	CN102	5.6	2.1
CN69	2.3	0.5	CN69	3.6	4.1
CN27	6.4	2.5	CN27	5.6	12.6
CN13	9.0	0.5	CN13	6.9	2.4
CN20	5.9	1.6	CN20	7.0	6.5
GTC2810	3.5	0.8	GTC2810	9.8	1.2
CN10	4.5	8.5	CN10	18.3	6.13
CN104	3.3	1.4	CN104	4.32	1.1
CN98	6.1	5.1	CN98	14.6	10.6
CN54	6.7	0.6	CN54	9.3	2.3
GTC2701	1.0	0.9	GTC2701	4.7	2.1
Amino- guanidine	3.9	1.2	Amino- guanidine	4.9	8.6

Overexpression of AGER-1 in fibroblasts treated with extracts SNB-GSS07, SNB-GSS04 and SNB-CN13 at 1µg/mL during 24 hours.

Protocol:

Cells were collected and solubilized in RIPA lysis buffer. Protein concentrations were determined using the BCA method. Equal amount of proteins (26 µg) were separated on SDS-PAGE and transferred on 0.45 µm PVDF membranes. The primary antibodies used were: monoclonal anti-vinculin antibody produced in mouse (Sigma-Aldrich #V9131), anti-DDOST (AGER-1) antibody produced in rabbit (Sigma-Aldrich #D6820). The following secondary antibodies were used: anti-mouse IRDye 800CW and anti-rabbit IRDye 680LT (LI-COR). Membranes were scanned with an Odyssey Imaging System (LI-COR). Quantification was performed using ImageJ software. Unnecessary lanes were cut off and demarcated using black line in the following figure.

Results:

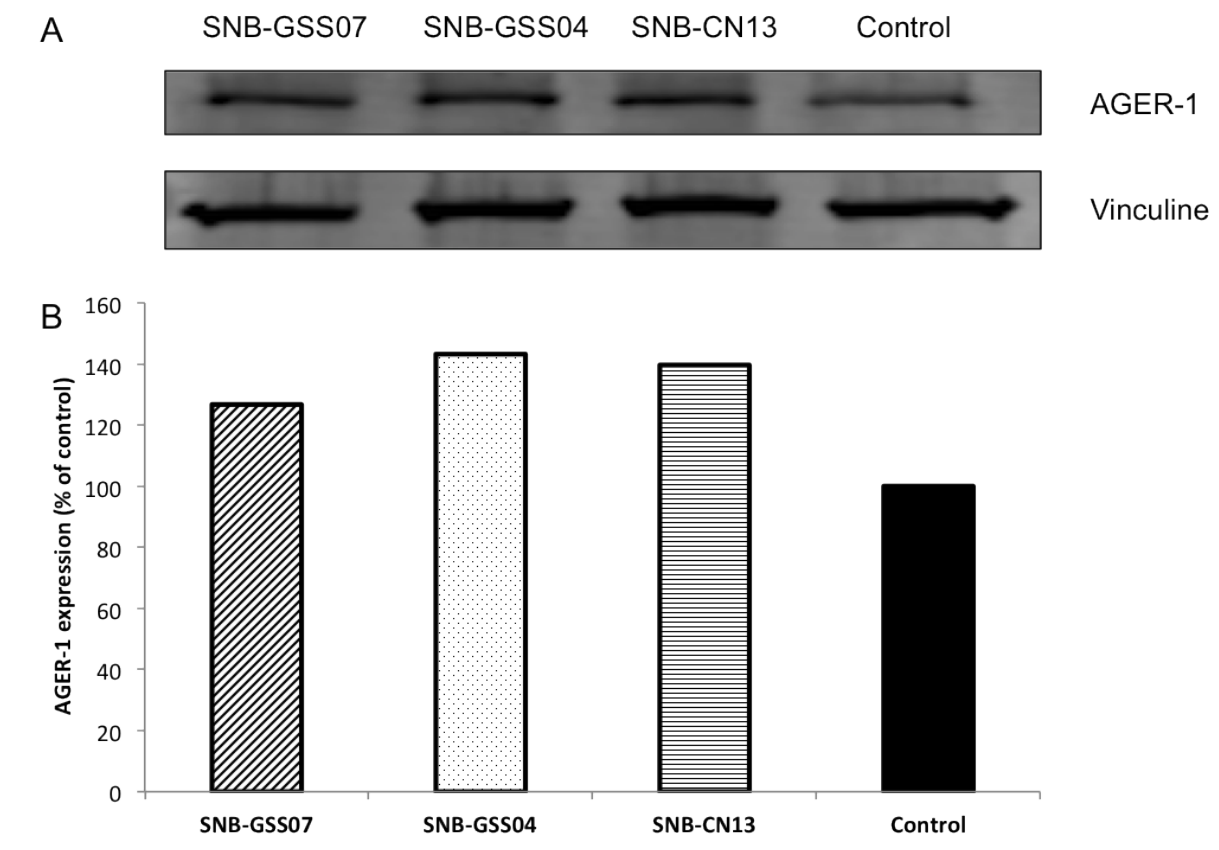


Figure S1. Overexpression of AGER-1 in fibroblasts treated with extracts SNB-GSS07, SNB-GSS04 and SNB-CN13 at 1µg/mL during 24 hours. (A) Total protein extracts of treated and control fibroblasts were analysed by western blotting using anti-AGER-1 antibody. Vinculin was used as loading control. (B) Quantification of AGER-1 expression in cells (data shown in A) and expressed as percentage of control.